Critical spin dynamics in $Nd_{1-x}Sr_xMnO_3$ with $x \approx 0.5$

V. V. Krishnamurthy* and I. Watanabe
The Institute of Physical and Chemical Research (RIKEN), Wako, Saitama 351-0198, Japan

K. Nagamine
The Institute of Physical and Chemical Research (RIKEN), Wako, Saitama 351-0198, Japan and Institute for Materials Structure Science, High Energy Accelerator Research Organization (KEK), Tsukuba, Ibaraki 305-0108, Japan

H. Kuwahara
Joint Research Center for Atom Technology (JRCAT), Tsukuba, Ibaraki 305-0044, Japan

Y. Tokura
Joint Research Center for Atom Technology (JRCAT), Tsukuba, Ibaraki 305-0044, Japan and Department of Applied Physics, University of Tokyo, Bonkyo-ku, Tokyo 113-0033, Japan

(Received 21 April 1998; revised manuscript received 10 March 1999)

Magnetic ion spin dynamics has been investigated in the perovskite manganite $Nd_{1-x}Sr_xMnO_3$ single crystals at the hole concentrations x of 0.5 and 0.55 by muon spin relaxation (μ^+SR) spectroscopy. We have observed the critical slowing down of Mn ion spin fluctuations on approaching the ferromagnetic ordering at ~ 251 K in $Nd_{0.5}Sr_{0.5}MnO_3$. The critical paramagnetic spin fluctuations, measured by the muon spin relaxation rate λ_1, exhibit a crossover behavior from exchange critical regime to dipolar critical regime. This crossover is explained by considering the suppression of longitudinal and transverse components of spin susceptibility by dipolar interactions closer to T_C and the dipolar vector q_D is found to be 0.020(2) Å^{-1}. The dynamic critical exponent $z = 2.00(12)$, deduced from muon spin relaxation rates away from T_C (nonasymptotic regime), agrees with the experimental and the theoretical results of $3d$ dipolar ferromagnets. Critical slowing down is not observed in the $x = 0.55$ crystal at the onset of antiferromagnetic ordering at ~ 220 K. Muon spin relaxation in the $x = 0.5$ crystal (above $T_N \approx 160$ K) and in the $x = 0.55$ crystal (both above and below T_N) is root exponential and indicates nondiffusive relaxation mechanism as is in a magnetic glass. The growth of a glasslike relaxation component concomitant with the magnetic ordering has been observed in both the crystals. We suggest that this glassy component originates from those Mn ions located in local regions containing small and differently sized spin clusters.

I. INTRODUCTION

The recent discovery of colossal magnetoresistance (CMR) in hole doped perovskite-type manganese oxides $R_{1-x}A_xMnO_3$ (R = Rare earth, e.g., La, Pr, Nd; A = divalent ion, e.g., Ca, Sr) has renewed the interest in their magnetic and structural properties.[1–4] The existence of metallic ferromagnetic ground state at moderate hole doping ($0.2 < x < 0.5$) in these mixed valent (Mn^{3+}, Mn^{4+}) manganites has been explained in the framework of the double exchange model.[5] The recently discovered CMR or magnetotransport at a paramagnetic insulator-to-ferromagnetic-metal transition has been suggested to be associated with the ferromagnetic double exchange interaction and lattice polarons which arise due to strong electron-phonon interaction caused by the Jahn-Teller distortion of the Mn^{3+} ion, in which out of the four unpaired electrons, three are in the t_{2g} states and one in the e_g state.[6] Growing evidence of lattice polarons in the insulating paramagnetic phase of $La_{1-x}Ca_xMnO_3$ ($x \sim 1/3, T_C \approx 250$ K) has been reported from a variety of experimental observations.[7,8] The electronic properties and the magnetic ground state of doped manganites are correlated with the e_g electron transfer interaction (t) or the one-electron bandwidth W_B which is determined by the radii of constituent ions and approximately equals to T_C. Extensive experimental and theoretical studies on the CMR manganites with the hole doping concentration x of $\sim 1/3$ have been reported in the literature.[1–10] At a similar bandwidth W_B and a higher hole doping x of ~ 0.5, the metallic ferromagnetism is unstable against charge ordering, i.e., the real space ordering of Mn^{3+} and Mn^{4+} ions in 1:1 ratio in the crystal, and an insulating antiferromagnetic ground state is realized. Therefore, it is interesting to study the intrinsic magnetic properties of the CMR manganites at the hole doping concentration $x \sim 0.5$, where both the ferromagnetic double exchange and the antiferromagnetic superexchange strongly contribute to the spin-spin interactions.

Recently, Kuwahara *et al.* discovered that single crystals of $Nd_{0.5}Sr_{0.5}MnO_3$ exhibit CMR at a magnetic-field-induced first-order phase transition from antiferromagnetic insulator-to-ferromagnetic metal.[11] On cooling, $Nd_{0.5}Sr_{0.5}MnO_3$ single crystals first undergo a second-order phase transition from paramagnetic-to-ferromagnetic state with $T_C \approx 251$ K. With further cooling, a first-order magnetic transition to antiferromagnetic state with CE-type structure occurs at the Néel temperature $T_N \approx 160$ K simultaneously with a metal-

insulator transition. The metal-insulator (MI) transition at ~ 160 K has been assigned to charge ordering of Mn^{3+} and Mn^{4+} ions in the crystal and is confirmed by neutron and electron diffraction measurements.[12,13] The CE-type antiferromagnetic structure is also accompanied by $(3z^2-r^2)$-type orbital ordering.[13] Further, the charge-ordered antiferromagnetic state collapses in an external magnetic field ($\sim$Tesla), and the insulating antiferromagnet transforms into a ferromagnetic metal. This effect has been interpreted as the melting of the charge-ordered state by the applied magnetic field. The crystal structure of $Nd_{0.5}Sr_{0.5}MnO_3$ above ~ 161 K is described by an orthorhombically ($Pbnm$) distorted perovskite lattice with the lattice constants $a=5.477(1)$ Å, $b=5.434(1)$ Å, and $c/\sqrt{2}=5.398(1)$ Å at 296 K.[11,12] $Nd_{0.45}Sr_{0.55}MnO_3$ is an *A*-type layered antiferromagnet with $T_N \sim 220$ K where it also undergoes a first-order structural phase transition.[12,14] $Nd_{0.45}Sr_{0.55}MnO_3$ crystal exhibits metallic behavior in the ferromagnetically coupled **ab** plane ([011]) and insulating behavior along the antiferromagnetically coupled **c** axis. Further, in the **ab** plane, (x^2-y^2) orbital ordering is expected to occur in this crystal. The spin-wave dispersion relations, measured by neutron scattering, show antiferromagnetic correlations along the [001] direction, whereas the correlations along the [110] direction are ferromagnetic with an excitation gap of 2.5–3 meV, suggesting a strong magnetic anisotropy in the crystal.[15] These results indicate that the magnetism, magnetotransport, and the phase diagram of $Nd_{1-x}Sr_xMnO_3$ crystals are highly complex. Further investigations of the magnetic transitions in $Nd_{1-x}Sr_xMnO_3$ crystals are highly desirable for a better understanding of the complex interplay between magnetism and magnetotransport properties. With this motivation, we have applied muon spin relaxation (μ^+SR) spectroscopy as a microscopic probe to investigate the spin dynamics of magnetic ions through the measurement of muon spin longitudinal relaxation rate λ across the magnetic phase transitions in the perovskite manganite system $Nd_{1-x}Sr_xMnO_3$ at $x=0.5$ and at $x=0.55$. Our μ^+SR measurements detect the critical slowing down of spin fluctuations of Mn ions in the critical paramagnetic regime in $Nd_{0.5}Sr_{0.5}MnO_3$. The muon spin-lattice relaxation rate λ_1 in this crystal exhibits a crossover from the exchange critical regime to the dipolar critical regime. The dynamic critical exponent *z* deduced from muon spin relaxation rates agrees with the theoretical and experimental *z* values of 3*d* dipolar ferromagnets. Nondiffusive or glass-type relaxation has been observed at the onset of magnetic ordering in some local regions of the crystals. Our μSR results strongly indicate that small spin clusters form in the high temperature paramagnetic state and a fraction of them remain in the low temperature magnetically ordered state.

This paper is organized as follows. In Sec. II, we briefly outline the preparation and the characterization of samples and the μ^+SR technique. Data analysis and the results of μ^+SR experiments in $Nd_{0.5}Sr_{0.5}MnO_3$ and $Nd_{0.45}Sr_{0.55}MnO_3$ are presented in Sec. III. The results of zero-field μ^+SR and longitudinal field μ^+SR in both crystals are further divided into subsections. In Sec. IV, we present the discussion of the results on spin dynamics in antiferromagnetic and/or ferromagnetic and the critical paramagnetic regions of the two crystals. Finally, the main findings of the present μ^+SR investigations are summarized in Sec. V.

II. EXPERIMENT

Single crystals of $Nd_{1-x}Sr_xMnO_3$ ($x=0.50$ and $x=0.55$) were grown from the stoichiometric mixture of constituent oxides Nd_2O_3, Mn_3O_4, and carbonate $SrCO_3$ by the floating-zone method with a procedure similar to that reported in Ref. 16. These crystals were characterized by x-ray diffraction, which showed that the samples are formed in single phase. Further, dc magnetization and dc magnetic susceptibility measurements were carried out to characterize the magnetic properties and the magnetic ordering temperatures (T_N or T_C) of both samples and were found to be within 5 K of the previously reported values.[11,12]

Positive muon spin relaxation[17] (μ^+SR) measurements were carried out using the μSR spectrometer at Port-2 of RIKEN-RAL muon facility,[18] Rutherford-Appleton Laboratory, Oxfordshire, United Kingdom. Each sample was a ~ 20 mmϕ mosaic of 5 mmϕ crystals of thickness 0.3 mm and was glued to a 25 μm thick silver plate. A pulsed beam [~ 80 ns full width at half maximum (FWHM) at a repetition rate of 50 Hz) of positive muons, polarized along their line of flight and having a momentum of 27 MeV/*c*, were implanted into the crystals of $Nd_{1-x}Sr_xMnO_3$ with $x=0.50$ and $x=0.55$. These muons are then depolarized by internal magnetic fields present in the samples. This depolarization is measured by monitoring the time evolution of the forward-backward asymmetry in the count of positrons emitted preferentially along the spin direction of the decaying muons (lifetime $\tau=2.2$ μs). A time-to-digital converter is started as the muon enters the target and stopped when the decay positron is detected in a scintillation detector array. From the time-dependent positron counting rates $F(t)$ and $B(t)$ measured respectively in the forward and backward detectors, the muon spin depolarization or relaxation function

$$P_Z(t)=\frac{(F-\alpha B)}{(F+\alpha B)} \tag{1}$$

is constructed. The normalization factor α, usually close to unity, corrects for the relative efficiencies of the forward and backward detectors. The consequences of the finite muon pulse width at RIKEN-RAL muon facility is that the time-dependent positron counting signals $F(t)$ and $B(t)$ are convoluted by the muon pulse function $r(t)$, which can be approximated by a Gaussian function of FWHM$\approx$80 ns. The effect of the convolution is to smear the signals in time, i.e., the actual measured signals would be $r(t)*F(t)$ and $r(t)*B(t)$. As a result of this convolution, the asymmetry of those muon spins which are coherently precessing in static internal magnetic fields greater than ~ 500 G will be lost from the measurement. Similarly, the convolution of the signals with the muon pulse function also affects the accuracy of the muon spin relaxation rates greater than ~ 20 μsec^{-1}. As will be seen in the following section, the muon spin relaxation rates measured in $Nd_{1-x}Sr_xMnO_3$ ($x=0.50$ and $x=0.55$) crystals are well below this limit; thus excluding the deconvolution of the positron counting signals is justified.

Muon spin relaxation spectra were measured at various temperatures in zero applied field, transverse field (20 G), and longitudinal field (100–3800 G) conditions. The measurements between 295 and 5 K were carried out in a flow-

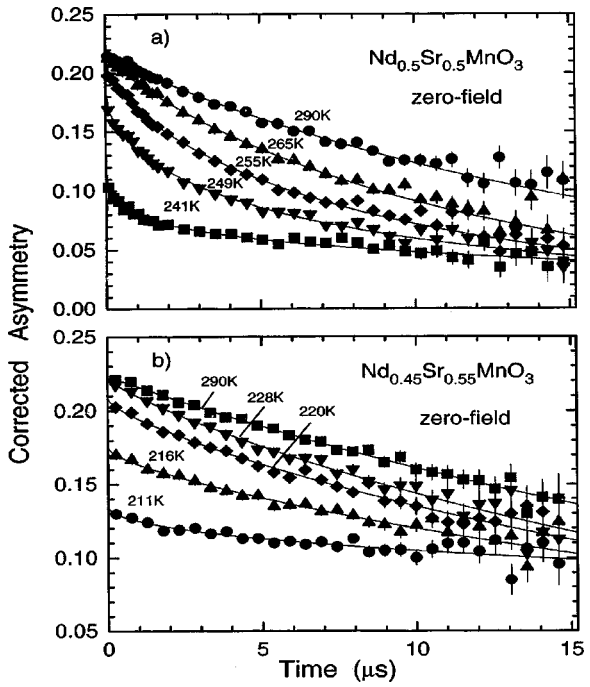

FIG. 1. (a) Muon spin relaxation (μ^+SR) spectra of $Nd_{0.5}Sr_{0.5}MnO_3$ crystal measured in zero-applied field, showing the paramagnetic to ferromagnetic phase transition at $T_C \approx 251$ K. (b) Muon spin relaxation spectra of $Nd_{0.45}Sr_{0.55}MnO_3$ crystal measured in zero-applied field near the paramagnetic to antiferromagnetic transition at $T_N \sim 220$ K. The solid lines show the best fits by the function described in Eq. (2).

type ^{4}He cryostat with a temperature stability of ± 60 mK at 250 K. Low temperature μ^+SR measurements between 1 and 2 K of $Nd_{0.5}Sr_{0.5}MnO_3$ sample were carried out in a ^{3}He cryostat.

III. RESULTS

A. Modeling of μ^+SR spectra and μ^+ stopping sites

Figure 1 shows some examples of μ^+SR spectra of $Nd_{0.5}Sr_{0.5}MnO_3$ and $Nd_{0.45}Sr_{0.55}MnO_3$ measured in zero applied field at a few selected temperatures below room temperature. Muon spin relaxation also occurs in longitudinal fields of 100–2000 G and suggests that the relaxation is dynamic in nature and electronic in origin. Let us first consider the possible stopping sites of μ^+ in $Nd_{1-x}Sr_xMnO_3$ ($x=0.5$ and $x=0.55$) crystals, to analytically represent the observed μ^+ spin relaxation spectral shape. In the case of high-T_C perovskite superconductors $RBa_2Cu_3O_{7-\delta}$ (R=rare earth such as Y or Gd), depending on the rare earth ion, 1 to 3 muon sites have been observed in the antiferromagnetic phase.[19] Generally, in the perovskite structure, such as that of $Nd_{1-x}Sr_xMnO_3$, muons are most likely to be located at 1 Å away from an oxygen ion due to their high affinity to form a O-μ^+ bond.[20] Considering that there are two (apical and planar) oxygen sites in the perovskite structure, two muon sites, one each at the apical oxygen and planar oxygen ions, are possible. Heffner *et al.*[9] have observed only one zero-field precession frequency for μ^+ in the ferromagnetic phase of perovskite manganite $La_{1-x}Ca_xMnO_3$. In the present μ^+SR measurements in $Nd_{1-x}Sr_xMnO_3$ ($x=0.5$ and $x=0.55$), we do not observe well-resolved multiple relaxation components due to crystallographically inequivalent muon sites in the muon spin relaxation spectra measured in the paramagnetic phases. The number of μ^+ stopping sites in the magnetically ordered states are assigned by considering the number of muon spin relaxation components required to obtain best fits of the data in the respective magnetic state of each crystal. In the following, we shall proceed to explain the best fitting functions obtained for different temperature regimes by considering the diffusive (defined by single correlation time τ_c) and nondiffusive (defined by a distribution of correlation times[21–23]) relaxation processes as well as the number of μ^+ stopping sites.

B. Zero-field μ^+SR in $Nd_{0.5}Sr_{0.5}MnO_3$

1. *Paramagnetic regime* ($T \geqslant T_C$)

Considering that there are no clear indications of multiple spin relaxation components in the muon spin relaxation spectra in the paramagnetic state as well as the lack of information on exact location and number of μ^+ sites in $Nd_{1-x}Sr_xMnO_3$, we have adopted a single site relaxation function for the paramagnetic phase. However, the spectra could not be fitted by one or more simple exponential $\exp(-\lambda t)$ relaxation functions at any given temperature, implying that the relaxation does not occur purely by spin diffusion defined by a single relaxation rate λ or a single spin-spin correlation time τ_c in the entire crystal. Thus, we have incorporated a root-exponential relaxation component $\exp(-\sqrt{\lambda t})$ to describe a diffusion-inhibited relaxation process due to a spatial distribution[21–23] of relaxation rates defined by a configurational average value of relaxation rate λ_2 in some local (glassy) regions of the crystal. The background contribution to the spectra was found to be negligibly small. Therefore, we model the μ^+SR spectra by the function

$$P_Z(t) = A_1 \exp(-\lambda_1 t) + A_2 \exp(-\sqrt{\lambda_2 t}), \qquad (2)$$

where A_1 is the asymmetry of the diffusive relaxation component and A_2 is the asymmetry of the nondiffusive relaxation component at time $t=0$ ($A_0 = A_1 + A_2$). In general, muon spin relaxation rate λ gives a measure of the fluctuating local magnetic field acting at the muon site due to the neighboring magnetic (Mn or Nd or both) ions through dipolar coupling, and is given by

$$\lambda = \gamma_\mu^2 \langle B_{loc}^2(0) \rangle \tau_c, \qquad (3)$$

where $\gamma_\mu = 2\pi \times 13.55$ kHz/G is the gyromagnetic ratio of the free muon, $B_{loc}(0)$ is the amplitude of the fluctuating local field felt by the muons at their stopping sites, and τ_c is the correlation time. The angular brackets represent the static equilibrium average of the square of the local magnetic field acting at the μ^+ site. The solid curves in Fig. 1 show the best fits to the data by Eq. (2). The asymmetry components A_1, A_2 and the total asymmetry A_0 obtained by fitting the μ^+SR spectra to Eq. (2) between 295 and 249 K are shown as a function of temperature in Fig. 2. The temperature dependencies of relaxation rates λ_1 and λ_2 are displayed in Fig. 3. We find that $\lambda_1 \equiv \lambda_2$ above T_C.

The features observed in the temperature dependence of A_0 and the various relaxation rate components in different

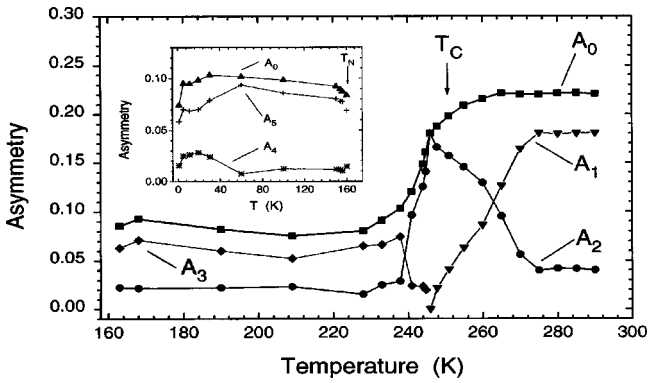

FIG. 2. Temperature dependence of the total asymmetry at $t=0$, A_0, the asymmetry of the exponential relaxation component A_e, and the asymmetry of the root-exponential relaxation components A_2 and A_3 in $Nd_{0.5}Sr_{0.5}MnO_3$. The solid lines are drawn to guide the eye.

temperature regions demonstrate the magnetic phase transitions occurring in the $x=0.5$ crystal. The total asymmetry A_0 of muons in $Nd_{0.5}Sr_{0.5}MnO_3$, plotted in Fig. 2, drops with the decrease of temperature between 251 and 210 K, showing the second-order phase transition from the paramagnetic to ferromagnetic state, observed in bulk magnetization measurements.[11] We would like to note that a small drop of asymmetry A_0 observed at 255 K should not be taken as the indication of the onset of magnetic ordering exactly at this temperature due to the limited time resolution of the pulsed muon beam, which could have strongly affected the spectra close to time $t=0$. The drop of A_1 and the increase of A_2 between 270 and 246 K display the loss of the diffusive component and the growth of the nondiffusive component, respectively.

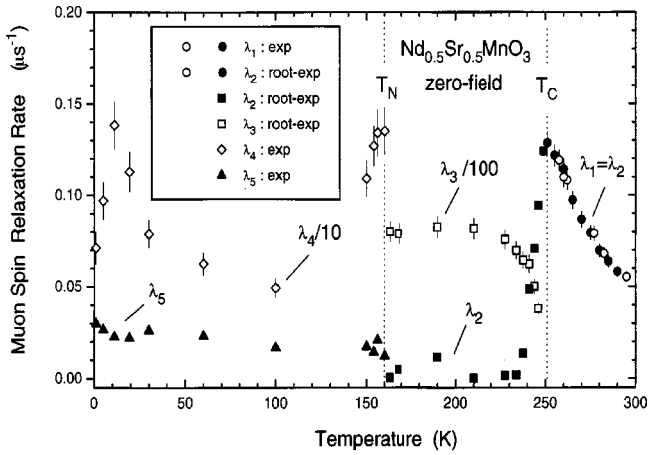

FIG. 3. The temperature dependence of muon spin relaxation rates. The filled circles (run 1) and open circles (run 2) show the temperature dependencies of λ_1 and λ_2 which illustrate the critical slowing down of Mn spin fluctuations above T_C in $Nd_{0.5}Sr_{0.5}MnO_3$. Open squares display the temperature dependence of the root-exponential relaxation component λ_3, having an asymmetry of A_3 in the ferromagnetic phase. λ_4 (open diamond) and λ_5 (filled triangles) display the temperature dependence of muon spin relaxation rates in the charge ordered CE-type antiferromagnetic state of $Nd_{0.5}Sr_{0.5}MnO_3$. For convenience of plotting, λ_3 and λ_4 are scaled by factors of 100 and 10, respectively. The dotted lines are drawn to guide the eye.

2. *Ferromagnetic regime* ($T \leqslant T_C$)

The muon spin relaxation spectra in the ferromagnetic state below ~ 251 K in $Nd_{0.5}Sr_{0.5}MnO_3$ could be best fitted with the muon spin relaxation function

$$P_Z(t) = A_2 \exp(-\sqrt{\lambda_2 t}) + A_3 \exp(-\sqrt{\lambda_3 t}), \qquad (4)$$

which contains only root exponential components, contrasted to the case of paramagnetic state described above. The resulting values of λ_2 and λ_3 are also included in Fig. 3. Based on the observed temperature dependence, we suggest that the faster component λ_3 originates from broadly distributed static local fields, mostly from the glasslike regions of the sample. The total asymmetry observed in the ferromagnetic state is given by $A_0 = A_2 + A_3$.

The asymmetry observed in the ferromagnetic state is much smaller than the value of total asymmetry A_0 observed in the paramagnetic state. At $0.84T_C$, where the asymmetry of the precessing part is expected to be saturated,[9] a fraction of asymmetry ($=7/11$) is lost in the ferromagnetic state. This fraction is associated with those muons precessing in the static local magnetic field present at their sites, due to the ferromagnetically ordered Mn moments, in the transverse direction with respect to initial muon polarization vector. The observed component of asymmetry ($A_0 = 4/11$) is due to depolarization or relaxation of the rest of the muons experiencing only a fluctuating local magnetic field parallel to their initial polarization vector. The observed splittings of 7/11 and 4/11 come out closer to the polycrystalline case, perhaps due to the smaller size of the single crystalline domain in the $x=0.5$ crystal.

The muon spin depolarization rate gives a measure of the spin-lattice relaxation rate of Mn ions experienced by muons at their interstitial sites via dipolar coupling. As shown in Fig. 3, the relaxation rate λ_2 in $Nd_{0.5}Sr_{0.5}MnO_3$ increases with the decrease of temperature from 295 K, reaches a maximum of $\sim 0.125(5)\ \mu s^{-1}$ in the range of 249 – 251 K, drops sharply at further lower temperatures and reaches a value of $\sim 0.04\ \mu s^{-1}$ at 228 K. The Curie temperature T_C of the $x=0.5$ crystal was determined from dc magnetization $M(T)$ data by (i) plotting the temperature derivative of magnetization $dM(T)/dT$ against temperature and (ii) the scaling analysis $M(T)$ vs $(T_C - T)^{\beta}$. The derivative $dM(T)/dT$ exhibits a maxima in the temperature interval of 249–252 K yielding a T_C^M of 251(1) K. The scaling analysis of magnetization was carried out by plotting $M(T)$ vs $(T_C - T)$ in a log-log plot. The T_C values in the above range of 249 to 252 K were found to return the best values 0.33(2) for the critical exponent β. More details of the scaling analysis of the static critical exponents, which serve as severe tests for the value of T_C, will be presented in Sec. IV. The maxima of the muon spin relaxation rate λ_2 in the range 249–251 K $\sim T_C^{\mu}$ agrees with the T_C^M determined from dc magnetization and T_C^{MI} of 251(2) K in electrical resistivity within the error. Further, the T_C (250 K) of $Nd_{0.5}Sr_{0.5}MnO_3$, reported from small angle neutron scattering measurements, also falls in this range.[24]

3. *Antiferromagnetic regime* ($T \leqslant T_N$)

Interestingly, in the charge-ordered antiferromagnetic state with CE-type structure below $T_{CO} \approx T_N \approx 160$ K, we

have observed two relaxation components, implying two magnetically inequivalent muon sites. Therefore, the μ^+SR spectra measured in the $Nd_{0.5}Sr_{0.5}MnO_3$ crystal between 160 and 1 K has been fitted by a function with two simple exponential relaxation components

$$P_Z(t) = A_4 \exp[-(\lambda_4 t)] + A_5 \exp[-(\lambda_5 t)], \qquad (5)$$

where A_4, A_5 are the asymmetries ($A_4 + A_5 = A_0$) and λ_4, λ_5 are the relaxation rates. The values of the initial asymmetry A_0 extracted by fitting the μ^+SR spectra of the $x = 0.5$ crystal for temperatures less than or equal to 160 K by Eq. (5) have been included in the plot of temperature versus asymmetry in Fig. 2. The temperature dependence of the relaxation rates λ_4 and λ_5 in the antiferromagnetic state of the $x = 0.5$ crystal are displayed in Fig. 3. At low temperatures ($\leqslant 60$ K), Nd^{3+} ions also contribute to the muon spin relaxation rates λ_4 and λ_5.

The initial asymmetry A_0, shown in Fig. 2, slightly increases on cooling from 163 to 150 K. This might be caused by the reorientation of ferromagnetically ordered Mn moments into the CE-type antiferromagnetic structure in relation to the first-order metal-insulator transition at ~ 160 K. The reorientation of Mn moments in $Nd_{0.5}Sr_{0.5}MnO_3$ between 161 and 150 K can alter the fractional muons which experience only parallel and only transverse magnetic field components with respect to the direction of initial polarization of muons. If more muons experience a local magnetic field parallel to their initial polarization vector in the antiferromagnetic state than in the ferromagnetic state, then this can account for the observed increase in asymmetry in the antiferromagnetic state. The occurrence of two magnetically inequivalent muon sites as evidenced by two muon spin relaxation components (λ_4 and λ_5) for temperatures $T \leqslant 160$ K is correlated with two simultaneous first-order transitions, a ferromagnetic to antiferromagnetic transition and a charge ordering transition at ~ 160 K. Such an observation is not unusual as the exchange energy contribution to the potential energy of a muon in the antiferromagnetic state is expected to be different from that in the ferromagnetic state and could have resulted in two magnetically inequivalent sites for the muons below $T_N \approx 160$ K.

The large values of λ_4 (see Fig. 3) close to 160 K are consistent with the onset of magnetic transition from ferromagnetic to antiferromagnetic transition at this temperature. At further lower temperatures, between 100 and 1 K, the relaxation rate λ_4 increases with the decrease of temperature and exhibits a broad peak which is centered around 11 K. The most likely sources of this low-temperature anomaly are (i) Nd-Mn exchange interaction which might have resulted in the canting of Mn spins and (ii) the magnetic ordering of Nd moments below 11 K. Considering the reduction of initial asymmetry A_0 (see Fig. 2) concomitant with the increase of relaxation rate λ_4 around 11 K and the lack of support for the canting of Mn spins from neutron scattering studies,[12] we attribute the anomaly at 11 K in the relaxation rates λ_4 of the $x = 0.5$ crystal to the magnetic ordering of Nd moments at ~ 11 K driven by an indirect RKKY exchange interaction between Nd ions. In contrast, the relaxation rates observed at the second muon site λ_5 are too small in magnitude and independent of temperature between 160 and 1 K, implying that the locations of those muons which contribute to λ_5 are relatively far from the magnetic Mn and Nd ions in the $Nd_{0.5}Sr_{0.5}MnO_3$ crystal. Further μ^+SR studies at a dc muon facility, where it would be possible to observe the spontaneous precession frequencies of muons in static local magnetic fields of several Tesla, are desirable to verify this point.

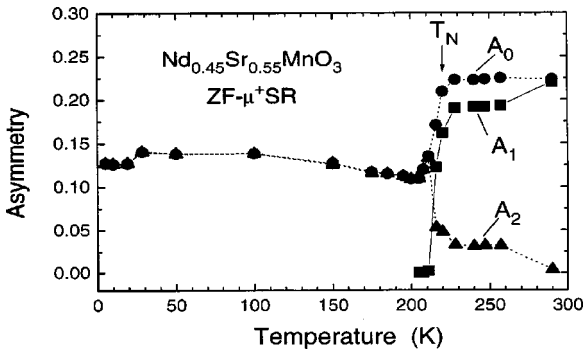

FIG. 4. Temperature dependence of the initial asymmetries A_0, A_1, and A_2 in $Nd_{0.45}Sr_{0.55}MnO_3$. The soild lines are drawn to guide the eye.

C. Influence of longitudinal fields on μ^+SR in $Nd_{0.5}Sr_{0.5}MnO_3$

In order to determine the static local magnetic field B_μ experienced by muons at their stopping sites in the magnetically ordered phases and the influence of longitudinal fields on the spin dynamics in $Nd_{1-x}Sr_xMnO_3$, we have carried out muon spin relaxation measurements in longitudinal fields in the range of 100 to 3800 G at 169 K in the ferromagnetic phase and at 60 K and 5.5 K in the antiferromagnetic phase of the $x = 0.5$ crystal. In all these measurements, most of the lost asymmetry component could not be recovered even at the highest available longitudinal field of 3800 G. Thus the internal fields are expected to be larger at least by a factor of 5, i.e., greater than 20 000 G. In the paramagnetic state of $Nd_{0.5}Sr_{0.5}MnO_3$, at 290 K, the relaxation rate shows a small drop with the applied field, i.e., $\sim 0.044\ \mu s^{-1}$ in zero applied field to $\sim 0.035\ \mu s^{-1}$ in longitudinal fields of 1000–3800 G, due to the decoupling of the nuclear dipolar relaxation, where as the asymmetries A_1 and A_2 remain constant at their respective zero-field values. Similarly, the muon spin relaxation rate λ_2 measured in the magnetically ordered phases at 169 and 5.5 K under the influence of longitudinal fields also drops slightly. The total asymmetry A_0 is also nearly unaffected by the applied field at the above temperatures.

D. μ^+SR in $Nd_{0.45}Sr_{0.55}MnO_3$

1. Spin dynamics in zero field

The μ^+SR spectra of the $x = 0.55$ crystal in zero applied field at all the measurement temperatures between 290 and 5 K could be fitted best by Eq. (2). The results of fit parameters A_1, A_2, and A_0 are plotted as a function of temperature in Fig. 4. The temperature dependencies of λ_1 and λ_2 are plotted in Fig. 5. As can be seen from Figs. 4 and 5, μ^+SR in the layered (A-type) antiferromagnet $Nd_{0.45}Sr_{0.55}MnO_3$ also shows anomalies in the temperature dependence of initial asymmetry A_0 and muon spin relaxation rate λ_2. The initial

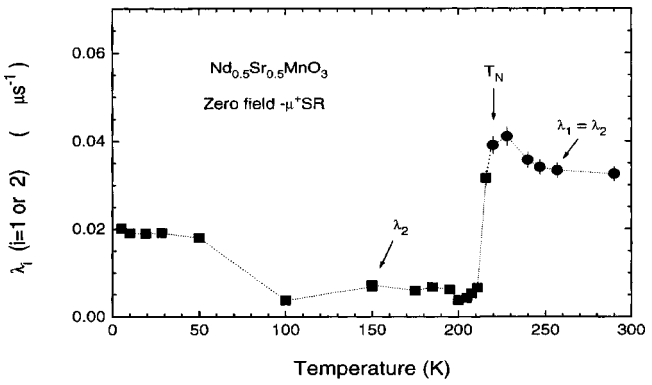

FIG. 5. Temperature dependence of muon spin relaxation rates λ_1 or λ_2 in $Nd_{0.45}Sr_{0.55}MnO_3$. The dotted line is a guide to the eye.

asymmetry A_0 starts to drop at ~ 220 K, consistent with the paramagnetic-to-antiferromagnetic transition with $T_N \approx 220$ K observed in the magnetic susceptibility and the anomaly in electrical resistivity at this temperature. A_0 decreases with the lowering of temperature between 220 and 200 K due to the loss of asymmetry from those muons precessing in the static local magnetic field in the antiferromagnetic state. We would like to note that the longituidinal and transverse components split into 1/2 and 1/2 in this $x=0.45$ crystal. A_0 slowly increases with decrease of temperature between 200 and 50 K. A small drop is observed in A_0 at ~ 20 K, whereas the relaxation rate saturates at this temperature. These features also seem to indicate the possible magnetic ordering of Nd sublattices below ~ 20 K, in similarity with the observations in $Nd_{0.5}Sr_{0.5}MnO_3$ discussed above. The relaxation rate λ_2 reaches a maximum of $\sim 0.038\ \mu s^{-1}$ at 228 K. Below 220 K, λ_2 drops to much smaller values. Interestingly, the relaxation rates show a small drop just above T_N and remain nearly temperature independent ($\lambda_1 = \lambda_2 \sim 0.031\ \mu s^{-1}$) between 240 and 290 K. The lack of a temperature dependence for λ_1 or λ_2 above T_N suggests that strong magnetic correlations are persistent even in the paramagnetic state. This result is consistent with the observation of short-range ferromagnetic order in neutron scattering.[15]

2. Spin dynamics in longitudinal fields

We have also carried out the experiments of longitudinal field decoupling of muon spin relaxation in $Nd_{0.45}Sr_{0.55}MnO_3$ at 50 and 5 K. Figure 6 displays the field dependence of λ_1 ($=\lambda_2$) and the asymmetries A_1 and A_2 obtained by fitting the longitudinal field μ^+SR spectra of $Nd_{0.45}Sr_{0.55}MnO_3$ to Eq. (2). At 50 K, the muon spin relaxation rate λ_2 increases with the application of the applied field. We believe that the increase of muon spin relaxation rate λ_2 with the longitudinal field could have been caused by a small rearrangement of spin configurations and the resulting frustration in applied fields. The asymmetry is redistributed between A_1 and A_2, with A_1 tending to increase and thus causing a drop in A_2. Interestingly, we find that $A_1 = A_2$ at 3800 G. The field-induced increase of A_2 indicates a tendency of change from nondiffusive to diffusive relaxation. These observations strongly indicate that the layered (A-type) antiferromagnet $Nd_{0.45}Sr_{0.55}MnO_3$ is more sensitive to small applied fields than the CE-type 3D antiferromagnet $Nd_{0.5}Sr_{0.5}MnO_3$. We

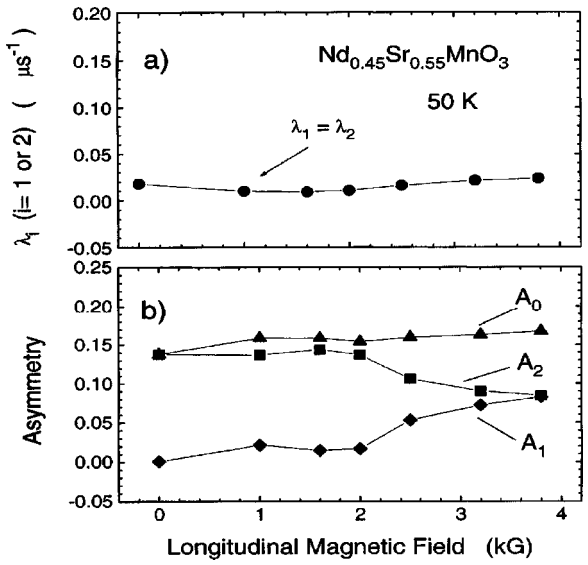

FIG. 6. Longitudinal field (0-3800G) dependence of muon spin relaxation rates λ_1, λ_2 and the initial asymmetries A_1, A_2, and A_0 in $Nd_{0.45}Sr_{0.55}MnO_3$ measured at 50 K.

have not observed any significant field dependence of μ^+SR at 5 K, implying that the applied longitudinal fields are too weak to influence the relaxation at low temperatures.

IV. DISCUSSION

A. Significance of relaxation processes

Usually, in an ideal ferromagnet and in some antiferromagnets, simple exponentially decaying muon spin relaxation functions have been observed. The exponential shape of the μ^+SR spectra is characteristic of a spin system relaxing via spin diffusion with a single relaxation rate λ. A simple exponential does not account for the entire asymmetry of the μ^+SR spectra of $Nd_{0.5}Sr_{0.5}MnO_3$ crystal and, as mentioned above, the inclusion of a root-exponential relaxation component is necessary to fit the spectra well. The root-exponential relaxation function describes the relaxation without spin diffusion and is usually observed in dilute spin glasses due to spatially averaging over the muon sites having different local configurations of surrounding electronic spins.[25] Apart from muon spin relaxation in dilute spin glasses, NMR relaxation in highly doped magnetic glasses is another case where root-exponential relaxation has been observed. From the present μSR study, we find that some of the perovskite manganites, for example the present system $Nd_{1-x}Sr_xMnO_3$, also fall in this category. Based on these similarities, we suggest that the root-exponential component is connected with the glasslike regions of the samples, which perhaps are related to the formation of spin clusters or polarons such as those observed in electron spin resonance and neutron scattering investigations of $La_{0.7}Ca_{0.3}MnO_3$ polycrystals.[7,8] In a recent μ^+SR study on another CMR material, $La_{0.7}Ca_{0.3}MnO_3$, Heffner *et al.* have also observed root-exponential relaxation in the ferromagnetic phase.[9] Nonexponential relaxation in the ^{139}La NMR of $La_{0.7}Ca_{0.3}MnO_3$ is also reported by Allodi *et al.*[26] We would like to note that the temperature dependence of the asymmetry of the root-exponential component A_2 (see Figs. 2 and 4)

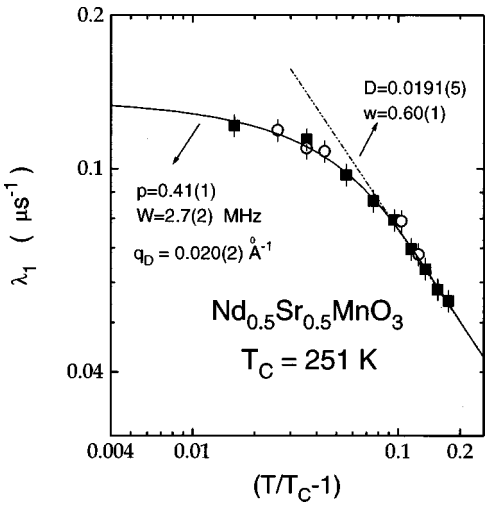

FIG. 7. Power law parametrization of the relaxation rates in $Nd_{0.5}Sr_{0.5}MnO_3$ for $T>T_C=251$ K showing the crossover behavior of the dynamic critical exponent *w*. The filled squares and the open circles represent the data taken from run 1 and run 2, respectively. The broken line shows the best fit for $t\geqslant 0.07$ by Eq. (6). The solid curve is a fit to the data by Eq. (11).

clearly demonstrates the growth of the glasslike regions concomitant with magnetic ordering in both $Nd_{0.5}Sr_{0.5}MnO_3$ and $Nd_{0.45}Sr_{0.55}MnO_3$ crystals in the present μ^+SR study. Our explanation for the temperature dependence of root-exponential relaxation and its origin is as follows. Small sized spin clusters form in the high-temperature paramagnetic phase, perhaps due to local variations in the arrangements of Mn^{3+} and Mn^{4+} charges. They grow in numbers as the crystal is cooled towards a magnetic transition. At T_C several of these clusters merge to form a large cluster and order ferromagnetically. Thus some local regions which contain variable sized small clusters seem to remain in the ordered state. When muons are located in such regions, they might experience root-exponential relaxation due to different spin-spin correlation times of individual clusters in that region.

The absolute values of muon spin relaxation rates (shown in Fig. 3) observed for temperatures $T\geqslant T_C$ in $Nd_{0.5}Sr_{0.5}MnO_3$ ($\sim 0.125\ \mu s^{-1}$ at T_C) and across T_N in $Nd_{0.45}Sr_{0.55}MnO_3$ ($0.04\ \mu s^{-1}$ at T_N) (shown in Fig. 5) are smaller compared to the muon spin relaxation rates observed near T_C in $La_{0.7}Ca_{0.3}MnO_3$ ($\sim 0.4\ \mu s^{-1}$ at T_C),[9] by a factor of ~ 3 ($x=0.5$), and ~ 10 ($x=0.55$) respectively. This means that the spin autocorrelation time τ_c is relatively higher in the La-based manganite.

B. Spin dynamics above T_C in $Nd_{0.5}Sr_{0.5}MnO_3$

Zero-field muon spin relaxation rates measured in $Nd_{1-x}Sr_xMnO_3$ ($x=0.5$ and $x=0.55$) crystals sensitively probe the spin dynamics at the second-order magnetic phase transitions as revealed by the appearance of anomalies at the corresponding transition temperatures. Let us consider the paramagnetic to ferromagnetic transition at 251 K in the $x=0.5$ crystal. At this transition, muon spin relaxation rates gradually increase with the decrease of temperature and show a divergence at ~ 251 K. This means, as the system is cooled towards its ferromagnetic ordering temperature, the paramagnetic spins form clusters, characterized by a correlation length ξ and exhibit critical slowing down. The temperature dependence of λ_1 for $T\geqslant T_C$ is associated with the dynamic critical phenomena,[27–29] i.e., the critical slowing down of spin fluctuations of Mn ions in the paramagnetic region closer to T_C. The critical paramagnetic spin fluctuations probed by zero-field muon spin relaxation measurements in ferromagnets are mostly sensitive to the fluctuation modes at small wave vectors **q**.[29,30,31]

In the general theory of scaling, the critical spin dynamics depends on the static universality class defined by the lattice dimensionality *d* and the order parameter dimensionality η. Each static universality class divides into separate dynamic subclasses depending on the additional perturbations. Different dynamics is expected depending on whether these perturbations are long range or short range, whether they conserve order parameter or not, and whether they involve anisotropy or not. The temperature dependence of λ_1, the exponentially relaxing (diffusive) component, in the critical paramagnetic region can be parametrized by a power law[29,32,33] of the form

$$\lambda_1(T)=Dt^{-w}, \tag{6}$$

where $t\equiv[(T/T_C)-1]$ is the reduced temperature, *D* is a proportionality constant, and *w* is the dynamic critical exponent for the diffusive component. The exponent *w* is given by the scaling law

$$w=\nu(z+2-d-\eta), \tag{7}$$

where *d* is the lattice dimensionality, *z* is the generalized dynamic critical exponent, ν is the static critical exponent, and η is the order-parameter dimensionality as defined in the general theory of scaling.[28] The exponent *z* gives a measure of rate of critical slowing down.[29] When the *t* range is restricted to $\approx 10^{-2}$, one obtains the asymptotic value of *z*. Following the approach of Suter *et al.* and Chow *et al.*,[34] we obtain the critical exponent *z* in the extended *t* region. Since our *t* values are greater than 10^{-2}, it should be noted that the value of *z* derived here corresponds to the nonaysmptotic regime. Small angle neutron scattering measurements of the temeprature dependence of correlation length ξ in $Nd_{0.5}Sr_{0.5}MnO_3$ above T_C have also proved critical spin dynamics and the critical exponent ν has been obtained in the reduced temperature range which extends up to 2×10^{-1}.[24] Following the dynamic scaling hypothesis of Ogielski for Ising spin glasses,[35] a configuration-averaged dynamic critical exponent $z_{av}=z/2$ can be defined for the root-exponential (glasslike) relaxation component.

In Fig. 7, the relaxation rates λ_1 for $T>T_C$ are plotted against the reduced temperature *t* in a log-log plot for the case of $T_C=251$ K. On cooling from high temperatures, the relaxation rate increases rapidly with decreasing *t* and shows critical spin fluctuations. At temperatures much closer to T_C, the increase of λ_1 is less steep and is indicative of a crossover in critical spin fluctuations from exchange regime to dipolar regime due to the influence of dipolar interactions between the spins. λ_1 values above T_C, i.e., for $0.07\leqslant t<0.16$, have been fitted by Eq. (6) for extracting the critical exponent *w* for the pure exchange critical region. The fitting yielded the critical exponent $w=0.60(1)$ and the proportion-

ality constant $D = 0.0191(5)\ \mu s^{-1}$. The fitted curve is displayed by a broken line in Fig. 7. To determine how the error in the determination of T_C affects the results of this reduced temperature plot, we have examined such plots by varying the T_C from 248 K to 255 K in steps of 1 K. If $T_C = 248$ K, the fitting by Eq. (6) resulted in $w = 0.60(1)$, $D = 0.0195(5)\ \mu s^{-1}$ for $0.075 \leqslant t \leqslant 0.16$. Similarly, if $T_C = 255$ K, the fitting results are $w = 0.55(1)$, $D = 0.0195(5)\ \mu s^{-1}$ for $0.065 \leqslant t \leqslant 0.16$. Therefore, by including the effects of error in the determination of T_C, we obtain the most appropriate value for the critical exponent as $w = 0.59(5)$ for the exchange critical regime ($T > 1.065 T_C$). The absolute value of the critical exponent w of $Nd_{0.5}Sr_{0.5}MnO_3$ is smaller compared to the theoretical value of 1.023(5) of the three-dimensional Heisenberg ferromagnet for the spin-conserved case, but closer to the value of 0.675(5) for the spin-non-conserved case.[36]

1. Critical exponents

Here we present a comparison of the static critical exponents of $Nd_{0.5}Sr_{0.5}MnO_3$ above T_C with those of $3d$ ferromagnets, either predicted by theoretical model calculations or determined from experiments. The magnetic susceptibility χ of $Nd_{0.5}Sr_{0.5}MnO_3$ obeys a power law $(T - T_C)^{\gamma}$ with $\gamma = 1.24(3)$ which, though smaller compared to the experimentally observed values of γ for isotropic ferromagnets such as 1.32 for Ni, 1.33 for Fe (Ref. 41), and the theoretical results of 1.375 for the $3d$ Heisenberg model, 1.318 for the $3d$ XY model, compares quite well with the result of 1.25 for the $3d$ Ising model from series expansions.[27] The dc magnetization M scales as $(T_C - T)^{\beta}$ with $\beta = 0.33(2)$, which shows deviation from the theoretical value of 0.38 for the $3d$ Heisenberg model, but agrees with the result of 0.312 for the $3d$ Ising model within the error. This β value also agrees with the experimental results of 0.33 for Ni and 0.34 for Fe. Further, the static critical exponents found in $Nd_{0.5}Sr_{0.5}MnO_3$, $\beta = 0.33(2)$ and $\gamma = 1.24(3)$, also agree with predictions of renormalization-group theory for three-dimensional anisotropic ferromagnet ($d = 3$, $n = 1$: model C).[29] The above values of β and γ are also consistent with the scaling law

$$\alpha + 2\beta + \gamma = 2 \tag{8}$$

if we assume $\alpha = 0.110$, which is a reasonable value for the $x = 0.5$ crystal.

Next we extract the dynamical critical exponent z of $Nd_{0.5}Sr_{0.5}MnO_3$ from the exponent w measured by μ^+SR. Using the value of 0.61(2) for the static critical exponent ν, determined by Rosenkranz *et al.*[24] from small-angle neutron-scattering measurements of the ferromagnetic transition at ~ 251 K in $Nd_{0.5}Sr_{0.5}MnO_3$, and $\eta = 0.031(4)$ of model C,[29] the value of $w = 0.59(5)$ and the scaling law of w given by Eq. (7) yield the generalized dynamical exponent z as 2.00(12) in the exchange critical region. The above z value deviates from the purely exchange-coupled isotropic Heisengerg model prediction of $z = 5/2$. This is not surprising, because the static critical exponents β and γ themselves do not agree with this model. The present μ^+SR result of dynamic cirical behavior in the $x = 0.5$ crystal is in a way supported by the recent theoretical investigations of the magnetic properties of the double exchange (DE) model by Zang *et al.*, who suggest that the low-energy excitations of the DE model are distinctly different from those of Heisenberg ferromagnets.[42] The experimental value of z for $Nd_{0.5}Sr_{0.5}MnO_3$ at the ferromagnetic transition marginally disagrees with the value of $z = 2.175(7)$ given by the scaling law

$$z = 2 + \alpha/\nu \tag{9}$$

for the $3d$ anisotropic ferromagnet (model C),[29] which, as shown above, is more suitable to describe the static critical phenomena at T_C in $Nd_{0.5}Sr_{0.5}MnO_3$. This small discrepancy could be due to fact that the wave vector $\mathbf{q}$ region probed in zero-field μ^+SR measurements is sensitive to the dipolar interactions between spins. However, the z of this crystal is in good agreement with the theoretical z value of 1.984(4) for dipolar ferromagnet (model A),[29] consistent with the strong influence of dipolar interactions on the critical paramagnetic spin fluctuations. The dynamic critical exponent z of $Nd_{0.5}Sr_{0.5}MnO_3$ also compares quite well with the z values of the isotropic ferromagnets EuO, EuS, Ni, and Co determined by hyperfine interaction techniques[29] such as the Mössbauer effect, nuclear magnetic resonance, and perturbed angular correlations. Bohn *et al.* have also reported a similar z of 2.09(6) for EuS from inelastic neutron scattering.[43]

2. Temperature dependence of muon spin relaxation rate λ_1 above T_C

Similar to the present case of $Nd_{0.5}Sr_{0.5}MnO_3$, a crossover in critical spin fluctuations has been observed in isotropic Heisenberg ferromagnets, for example, Fe, Ni, EuO, and EuS, and is associated with the crossover from the exchange critical regime away from T_C to dipolar critical regime closer to the T_C.[33,37–40] Far above T_C, both the longitudinal and transverse susceptibilities $\chi^{\parallel}(\mathbf{q})$ and $\chi^{\perp}(\mathbf{q})$ contribute equally to the magnetic ion spin dynamics. Close to T_C, the dipole interactions induce an anisotropy of the susceptibility with respect to $\mathbf{q}$. In mean-field theory, this corresponds to the following demagnetization correction to the Ornstein-Zernicke susceptibility expression:

$$[\chi^{\alpha\beta}(\mathbf{q} \rightarrow 0)] \propto \frac{q^{\alpha} q^{\beta}}{q^2} \tag{10}$$

($\alpha, \beta = x, y$, or z). Closer to the T_C, this extra term strongly suppresses the susceptibility due to longitudinal fluctuations $\chi^{\parallel}(\mathbf{q})$ from diverging at T_C, whereas that of the transverse fluctuations $\chi^{\perp}(\mathbf{q})$ are affected less severely[31,37] as shown in Fig. 1 of Ref. 30. Following Yaouanc *et al.*,[33] the longitudinal muon spin relaxation rate can be expressed as

$$\lambda_1 = W[2p^2 I^T(\psi) + (1-p)^2 I^L(\psi)], \tag{11}$$

where W is a nonuniversal constant and p is a material-dependent parameter. $\psi = \arctan(q_D \xi)$ is a measure for the temperature through its dependence on the correlation length ξ. The parameter q_D is the dipolar vector determined by the relative strengths of the dipolar and exchange interactions. $I^L(\psi)$ and $I^T(\psi)$ describe the contributions to λ_1 from longitudinal and transverse fluctuation modes, respectively. The application of mode-coupling theory for the $Nd_{0.5}Sr_{0.5}MnO_3$ crystal is justified, since there are no short-range antiferro-

magnetic correlations above T_C in this crystal, unlike in layered magnets of manganites. Using the above equation, with W, p, and q_D as free parameters, and taking $\xi_0 = 3.0$ Å from the small-angle neutron-scattering data of Ref. 24, a robust curve fit to the data of Fig. 7 could be obtained. The fit which is shown by the solid curve in Fig. 7 yielded the values of $W = 2.7(2)$ MHz, $p = 0.41(1)$, and $q_D = 0.020(2)$ Å^{-1}. This q_D value is intermediate to the q_D values of the isotropic ferromagnets, Ni (0.013 Å^{-1}) and Fe (0.033 Å^{-1}). Therefore, the ferromagnetic state originating from the double interaction in $Nd_{0.5}Sr_{0.5}MnO_3$ crystal is in a way similar to the one in the isotropic ferromagnets such as Fe, Ni, and EuS.

C. Spin dynamics near T_N in $Nd_{0.45}Sr_{0.55}MnO_3$

Ususally, the muon spin relaxation rate is expected to drop to nearly identical values on both sides of the peak value at the ordering temperature (in this case T_N) in a magnetic material. But, the relaxation rates measured above the Nèel temperature $T_N \sim 220$ K in $Nd_{0.45}Sr_{0.55}MnO_3$ are much higher (by a factor of 5) than those below T_N. They are also nearly temperature independent above T_N, i.e., they do not exhibit dynamic critical behavior as is observed in $Nd_{0.5}Sr_{0.5}MnO_3$. The absence of critical slowing down above T_N in $Nd_{0.45}Sr_{0.55}MnO_3$ seems to be related to the presence of short-range ferromagnetic correlations in the paramagnetic state of this material.[15] When ferromagnetic short-range correlations develop at a temperature much higher than T_N, the spin fluctuations will be reduced causing an enhancement of muon spin relaxation rates λ_1 or λ_2 at temperatures even far above from T_N. Another explanation is that the critical slowing down of spin fluctuations could be characteristic for materials with an order-disorder transition in the charge degrees of freedom. A comparative study of critical spin dynamics in colossal magnetoresistive manganites exhibiting charge ordering and those which do not exhibit charge ordering would be desirable for a further understanding of the possible relation between critical slowing down phenomena and charge ordering in CMR magnets.

V. CONCLUSIONS

In conclusion, we have microscopically investigated the spin dynamics at magnetic phase transitions in the colossal magnetoresistive oxide single crystals of $Nd_{1-x}Sr_xMnO_3$ at carrier doping concentrations of $x = 0.5$ and $x = 0.55$ using muon spin relaxation. The critical slowing down of Mn spin fluctuations has been observed above the ferromagnetic ordering temperature of 251 K in $Nd_{0.5}Sr_{0.5}MnO_3$. Muon spin relaxation rates above the Néel temperature of ~ 220 K in $Nd_{0.45}Sr_{0.55}MnO_3$ do not show critical slowing but indicate short-range magnetic correlations. The temperature dependence of muon spin relaxation rate λ_1 in $Nd_{0.5}Sr_{0.5}MnO_3$ in the critical paramagnetic region is quantitatively accounted within the mode-coupling theory of Yaouanc *et al.*[33] by considering the suppression of longitudinal and transverse components of spin susceptibility by dipolar interactions closer to T_C. The dipolar vector q_D is found to be 0.020(2) Å^{-1}. The dynamic critical exponent $z = 2.00(12)$, deduced from muon spin relaxation rate λ_1, agrees well with the experimental and the theoretical results for $3d$ dipolar ferromagnets such as Ni and EuS.[33] The observations of root-exponential relaxation components and the temperature dependence of their weights in μ^+SR show how spin-glass-type regions develop into the magnetically ordered states of $Nd_{1-x}Sr_xMnO_3$ crystals. Thus, using the μSR technique, we have demonstrated the spin dynamics of magnetic ions, the formation of small spin clusters, and their dependence on the carrier concentration around $x = 0.5$ in colossal magnetoresistive $Nd_{1-x}Sr_xMnO_3$ crystals.

ACKNOWLEDGMENTS

The authors would like to thank Professor T. P. Das, Professor J. Mydosh, Dr. H. Kawano, Dr. A. Asamitsu, Dr. Y. Tomioka, and Dr. I. P. Goudemond for very helpful discussions. They also thank the related staff of RAL for the smooth operation of the accelerator during the experiment. The part of the research work done at Joint Research Center for Atom Technology (JRCAT) is supported by the New Energy and Industrial Technology Development Organization (NEDO) of Japan. V.V.K. would like to acknowledge the support from RIKEN at Wako during the course of this work.

*Present address: SPring8, The Institute of Physical and Chemical Research (RIKEN), 1-1-1 Kouto, Mikazuki-cho, Sayo-gun, Hyogo 679-5148, Japan.
Electronic address: krishna@spring8.or.jp

[1] S. Jin, T. H. Tiefl, M. McCormack, R. A. Fastnacht, R. Ramesh, and L. H. Chen, Science **264**, 413 (1994).
[2] Y. Tokura, A. Urashibara, Y. Moritomo, T. Arima, A. Asamitsu, G. Kido, and N. Furukawa, J. Phys. Soc. Jpn. **63**, 3931 (1994).
[3] P. Schriffer, A. P. Ramirez, W. Bao, and S. W. Cheong, Phys. Rev. Lett. **75**, 3336 (1995).
[4] H. Kawano, R. Kajimoto, M. Kubota, and H. Yoshizawa, Phys. Rev. B **53**, R14 709 (1996).
[5] C. Zener, Phys. Rev. **82**, 403 (1951); P. W. Anderson and H. Hesegawa, *ibid.* **100**, 675 (1955); P. -G. de Gennes, *ibid.* **118**, 141 (1960).
[6] A. J. Mills, P. B. Littlewood, and B. I. Shraiman, Phys. Rev. Lett. **74**, 5144 (1995).
[7] Guo-meng Zhao, K. Conder, H. Keller, and K. A. Müller, Nature (London) **381**, 676 (1996); A. Shengelaya, Guo-meng Zhao, H. Keller, and K. A. Müller, Phys. Rev. Lett. **77**, 5296 (1996); Guo-meng Zhao, M. B. Hunt, and H. Keller, *ibid.* **78**, 955 (1997).
[8] S. J. L. Billinge, R. G. diFrancesco, G. H. Kwei, J. J. Neumeier, and J. D. Thompson, Phys. Rev. Lett. **77**, 715 (1996).
[9] R. H. Heffner, L. P. Le, M. F. Hundley, J. J. Neumeier, G. M. Luke, K. Kojima, B. Nachumi, Y. J. Uemura, D. E. MacLaughlin, and S-W. Cheong, Phys. Rev. Lett. **77**, 1869 (1996).
[10] L. Sheng, D. Y. Xing, D. N. Sheng, and C. S. Ting, Phys. Rev. Lett. **79**, 1710 (1997).
[11] H. Kuwahara, Y. Tomioka, A. Asamitsu, Y. Moritomo, and Y.

Tokura, Science **270**, 961 (1995).
[12] H. Kawano, R. Kajimoto, H. Yoshizawa, Y. Tomioka, H. Kuwahara, and Y. Tokura, Phys. Rev. Lett. **78**, 4253 (1997).
[13] J. Q. Li, Y. Matsui, H. Kuwahara, and Y. Tokura (private communication).
[14] H. Kuwahara (private communication).
[15] H. Yoshizawa, H. Kawano, J. A. Ferndandez-Beca, H. Kuwahara, and Y. Tokura, Phys. Rev. B **58**, R571 (1998).
[16] H. Kuwahara, Y. Moritomo, Y. Tomioka, A. Asamitsu, M. Kasai, R. Kumai, and Y. Tokura, Phys. Rev. B **56**, 9386 (1997).
[17] For a detailed description of the experimental methods of μSR, see A. Schenck, *Muon Spin Rotation Spectroscopy* (Adam Hilger Ltd., Bristol, 1985).
[18] K. Nagamine *et al.*, Hyperfine Interact. **101/102**, 521 (1996); RIKEN-RAL muon facility Report, Vol. 1 (1997).
[19] N. Nishina and H. Miyatake, Hyperfine Interact. **63**, 183 (1990).
[20] S. B. Sulaiman, S. Sreenivas, N. Sahoo, F. Hagelberg, T. P. Das, E. Torikai, and K. Nagamine, Phys. Rev. B **49**, 9879 (1993).
[21] I. J. Lowe and D. Tse, Phys. Rev. **166**, 279 (1968).
[22] D. Tse and S. R. Hartmann, Phys. Rev. Lett. **21**, 511 (1968).
[23] I. P. Goudemond, J. M. Keartland, M. J. R. Hoch, and G. A. Sounders, Phys. Rev. B **56**, R8463 (1997).
[24] S. Rosenkranz, R. Osborn, J. F. Mitchell, U. Geiser, J. Ku, A. J. Schultz, and D. M. Young, Physica B **241-243**, 448 (1998).
[25] Y. J. Uemura, T. Yamazaki, D. R. Harshman, M. Senba, and E. J. Ansaldo, Phys. Rev. B **31**, 546 (1985).
[26] G. Allodi, R. De Renzi, and G. Guidi, Phys. Rev. B **57**, 1024 (1998).
[27] S. K. Ma, *Modern Theory of Critical Phenomena* (Addision-Wesley, California, 1976).
[28] P. C. Hohenberg and B. I. Halperin, Rev. Mod. Phys. **49**, 435 (1977).
[29] For a compilation of various critical exponents and for a detailed review on the critical phenomena studied by nuclear techniques, see H. Hohenemser, N. Rosov, and A. Kleinhammes, Hyperfine Interact. **49**, 267 (1989).
[30] P. Dalmas de Reotier, A. Yaouanc, and E. Frey, Phys. Rev. B **50**, 3033 (1994).
[31] M. E. Fisher and A. Aharony, Phys. Rev. Lett. **30**, 559 (1973); Phys. Rev. B **8**, 3342 (1973).
[32] G. S. Collins, A. Chowdhury, and C. Hohenemser, Phys. Rev. B **33**, 4747 (1986); A. Chowdhury, G. S. Collins, and C. Hohenemser, *ibid.* **30**, 6277 (1984); **33**, 5070 (1986).
[33] A. Yaouanc, P. Dalmas de Reotier, and E. Frey, Phys. Rev. B **47**, 796 (1993).
[34] R. M. Suter and H. Hohenemser, Phys. Rev. Lett. **41**, 705 (1978); L. Chow, H. Hohenemser, and R. M. Suter, *ibid.* **45**, 908 (1980).
[35] A. T. Ogielski, Phys. Rev. B **32**, 7384 (1985).
[36] E. Frey and F. Schwabl, Adv. Phys. **43**, 577 (1994); E. Frey, F. Schwabl, S. Henneberger, O. Hartmann, R. Wappling, A. Kratzer, and G. M. Kalvius, Phys. Rev. Lett. **79**, 5142 (1997).
[37] J. Kötzler, Phys. Rev. Lett. **51**, 833 (1983).
[38] J. Kötzler, D. Görlitz, F. Mezei, and B. Farago, Europhys. Lett. **1**, 12 (1986).
[39] J. Kötzler, Phys. Rev. B **38**, R12 027 (1988); M. W. Pieper, J. Kötzler, and K. Nehrke, *ibid.* **47**, 11 962 (1993).
[40] K. Nishiyama, Y. Yagi, K. Ishida, T. Matsuzaki, K. Nagamine, and T. Yamazaki, Hyperfine Interact. **17**, 473 (1984).
[41] N. W. Ashcroft and N. D. Mermin, *Solid State Physics* (Halt, Rinehart and Winston, Philadelphia, 1976).
[42] J. Zang, H. Röder, J. R. Bishop, and S. A. Trugman, J. Phys.: Condens. Matter **9**, L157 (1997).
[43] H. G. Bohn, A. Kollmar, and W. Zinn, Phys. Rev. B **30**, 6504 (1984).